Quantum Electronics **43** (1) 14–20 (2013)

NONLINEAR OPTICAL PHENOMENA

PACS numbers: 42.70.Nq; 42.65.Wi; 71.36.+c
DOI: 10.1070/QE2013v043n01ABEH014913

Characteristics of surface photorefractive waves in a nonlinear SBN-75 crystal coated with a metal film

D.Kh. Nurligareev, B.A. Usievich, V.A. Sychugov, L.I. Ivleva

Abstract. **Based on the calculation of the electrostatic field potential of space charges, we have analysed the characteristic features of light-induced scattering of extraordinary polarised light in photorefractive (PR) crystals (for example, an SBN-75 crystal). Using the method of images, the electrostatic field is analysed for surface (aperiodic) waves along the crystal–dielectric (air) interface. It is shown that the field distributions satisfying the boundary conditions can emerge only upon accumulation of a screening electric charge in a narrow transition layer of thickness ~1 μm, the sign of the charge being opposite that of the space charge in the illuminated region of the crystal. A model is proposed to explain the observed features of the surface PR waves in a metal-film coated PR crystal. In considering the contact potential difference at the PR crystal–film interface it is shown that in the crystal layer (adjacent to the film) enriched with charge carriers, i.e., electrons, the refractive index can be significantly reduced. In the case of small excitation angles (0 – 1.5°), this layer can act as an optical barrier, the reflection from which can result in near-surface waves; a characteristic difference from the previously observed oscillatory surface waves is the presence of a broadened intensity distribution shifted inside the crystal.**

Keywords: *photorefractive crystal, nonlinear surface waves.*

1. Introduction

At present, intensive studies of nonlinear surface waves which started in the late twentieth century are being continued [1–3]. The most attractive feature of a photorefractive (PR) surface wave is the concentration of the energy of a light beam in a narrow surface layer, which can significantly increase the performance of PR devices, the fabrication of which does not require producing a waveguide structure in advance. When a PR surface wave is excited, one can expect an extraordinary enhancement of nonlinear optical effects, such as luminescence of molecules adsorbed on the crystal surface, Raman scattering, optical second harmonic generation, etc.

In papers [4, 5] we have shown experimentally that nonlinear surface waves can be excited not only at the crystal (SBN-75) – air interface, but also in the case when the active surface of the crystal is coated with an electrode, such as a layer of aquadag or silver. This opens up the possibility of investigating the new properties of the surface wave, which appear upon application of an external electric field to the crystal. Nevertheless, many important practical issues still remain to be clarified, in particular the mechanism of formation of a nonlinear PR wave with an aperiodic intensity profile, excited at the boundary of a metal-coated crystal.

The aim of the present work is an attempt to analyse the features of PR waves in a nonlinear SBN-75 crystal, which is adjacent to a dielectric (air) or coated with a metal film. We have shown that the material properties of the medium, which borders the crystal, can significantly affect the photoinduced scattering and field profile of the nonlinear waves excited at grazing incidence of the focused extraordinary polarised light beam from a 0.44-μm He–Cd laser. Based on the results obtained, we have proposed a model that describes the features of the PR surface waves in a metal-film coated SBN-75 crystal.

D.Kh. Nurligareev, B.A. Usievich, V.A. Sychugov, L.I. Ivleva
A.M. Prokhorov General Physics Institute, Russian Academy of Sciences, ul. Vavilova 38, 119991 Moscow, Russia;
e-mail: borisu@kapella.gpi.ru, jamil@kapella.gpi.ru

Received 25 June 2012; revision received 20 August 2012
Kvantovaya Elektronika **43** (1) 14–20 (2013)
Translated by I.A. Ulitkin

2. Electrostatic field of the space charges in propagation of a narrow light beam in a PR crystal

Let the polar axis of the crystal, c, unlimited in the plane xy, be oriented along the x axis, an extraordinary polarised (TM) light beam be distributed along the z axis and its intensity $I(x)$ be independent of the coordinate y. It is known that as a result of photoexcitation and spatial redistribution of charge carriers, i.e., electrons, nonuniform illumination of the PR crystal leads to the formation of space charge regions in the crystal. Within the zone transfer model, formulas for calculating the distributions of the space-charge density $\rho(x)$ and field $E_{sc}(x)$ in the steady state in a crystal with a partially compensated donor level and one type of carriers are presented in [6].

The space-charge field can also be expressed as the gradient of the electrostatic potential $\varphi(x)$:

$$E_{sc}(x) = -\,d\varphi(x)/dx. \tag{1}$$

By introducing the notation $\varphi_B = k_B T/e$ (T is the crystal temperature, and e is the elementary charge) and assuming $\varphi(\infty) = 0$, we write

$$\varphi(x) = \varphi_B \ln[1 + I(x)/I_d], \tag{2}$$

where I_d is the dark illumination intensity. According to (2), a potential profile $\varphi(x)$ corresponds to the given distribution $I(x)$ in an unlimited PR crystal. Conversely, for the given distribution $\varphi(x)$ the condition of the stationary distribution of electrical charges in the crystal is given by the intensity profile of the light wave

$$I(x) = I_d \exp[\varphi(x)/\varphi_B - 1]. \quad (3)$$

Nonlinear addition $\Delta n(x)$ to the unperturbed refractive index n_2 of the crystal has the form

$$\Delta n(x) = -(1/2) n_2^3 r_{eff} E_{sc}(x), \quad (4)$$

where r_{eff} is the effective electro-optic coefficient.

Figure 1 shows the distributions $\varphi(x)$, $E_{sc}(x)$, $\rho(x)$ and $\Delta n(x)$, calculated for a Gaussian beam with an intensity $I(x) = I_0 \exp(-x^2/w_0^2)$ (I_0 is the intensity on the beam axis, and w_0 is the beam radius) at $w_0 = 100$ μm, the dielectric constant of the crystal $\varepsilon = 2500$, $r_{eff} = 750$ pm V^{-1}, and different ratios I_0/I_d. Extreme values of $\pm E_m$ and $\pm\Delta n_m$ of $E_{sc}(x)$ and $\Delta n(x)$ are reached for $\rho(x) = 0$ at points $x = \pm x_m$, satisfying the condition

$$I(x_m)/I_d = 2x_m^2/w_0^2 - 1. \quad (5)$$

According to the calculations, with increasing ratio I_0/I_d the positive charge, concentrated between the points $x = \pm x_m$, noticeably increased, though the maximum concentration of the charge $N_d^+ \sim (1-2) \times 10^{12}$ cm^{-3}, which is reached on the beam axis [$\rho(0) = \rho_m = 2\varepsilon\varepsilon_0(\varphi_B/w_0^2) I_0/(I_0 + I_d)$], is much less than the effective concentration of the traps for the studied SBN crystal ($N_{eff} \sim 10^{16}-10^{17}$ cm^{-3} [7]).

The dependences $\Delta n(x)$ in Fig. 1d demonstrates a linear central and a nonlinear peripheral parts. It can be seen that the value of Δn_m increases noticeably with increasing beam intensity at a fixed background illumination. In this case, the region of the crystal with a linear dependence $\Delta n(x)$ is greatly extended, and the regions with a nonlinear dependence $\Delta n(x)$, localised in the vicinity of the extrema, are shifted to the periphery of the beam, where $I(x) \ll I_0$. Distortions of the wave surfaces of the beam, associated with the nonlinearity of $\Delta n(x)$ in the region of extrema, should manifest themselves in this case to a lesser degree.

These results are consistent with the results of paper [8], which analysed the propagation of a Gaussian beam in a photorefractive $BaTiO_3$ crystal. In assessing the influence of the optical inhomogeneities on the propagating beam, Feinberg [8], selecting the central part of the linear profile $\Delta n(x)$, noted that the region of the crystal, corresponding to the central part of the beam, works as a prism, which rotates the beam. According to the calculations [8], when the intensity maximum is shifted from the beam axis in the direction which is opposite to the axis of the beam direction, there appear a dip in the intensity distribution and a second maximum. A similar situation was observed in our experiments when the SBN-75 crystal was exposed to the Gaussian light beam for a short time (~1 s) [5]. We assume that for the part of the beam corresponding to the region of positive $\Delta n(x)$, the propagation regime is realised, which is similar to the propagation of solitons in an SBN crystal in the presence of an external field [9]. Spatial solitons are usually observed in PR crystals with an

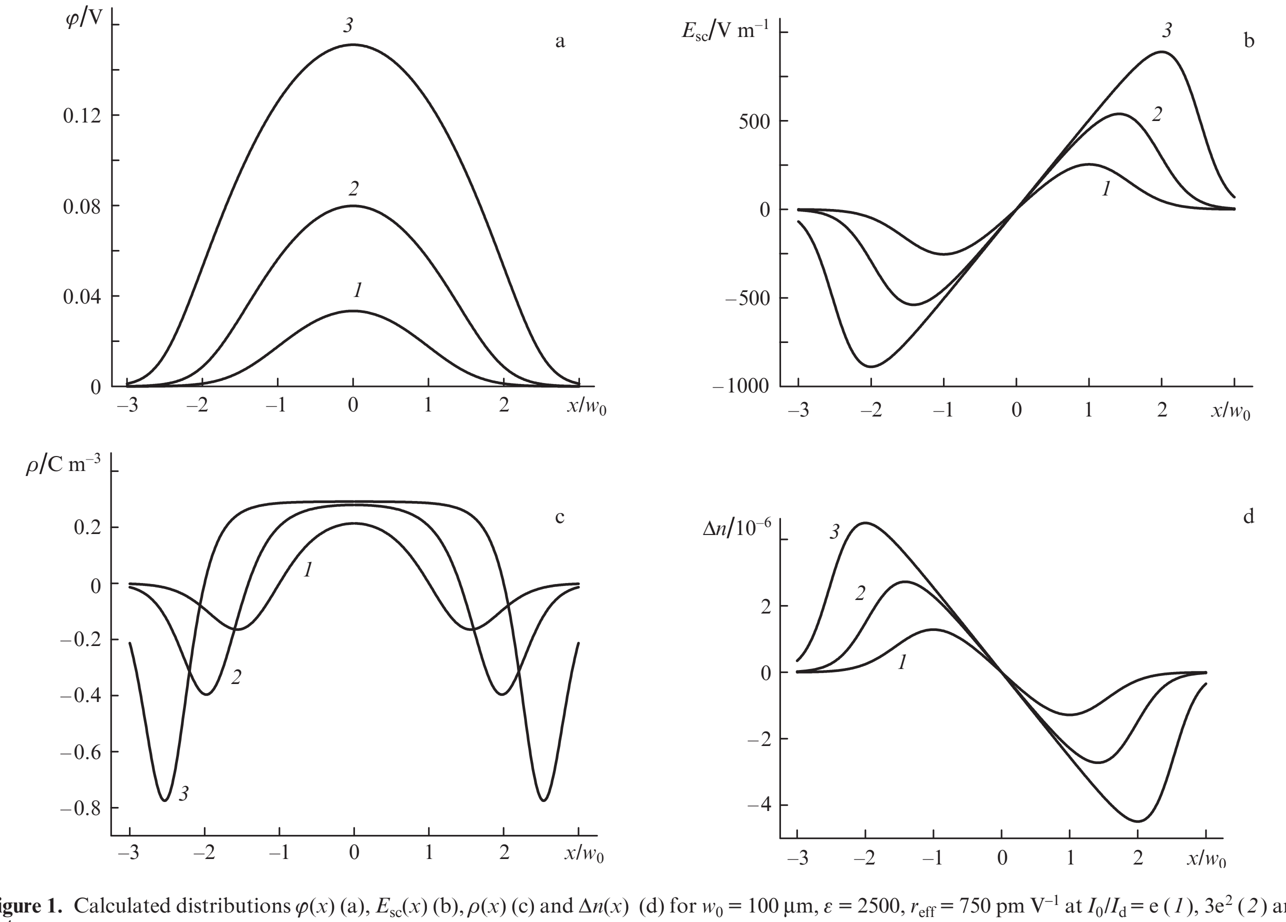

Figure 1. Calculated distributions $\varphi(x)$ (a), $E_{sc}(x)$ (b), $\rho(x)$ (c) and $\Delta n(x)$ (d) for $w_0 = 100$ μm, $\varepsilon = 2500$, $r_{eff} = 750$ pm V^{-1} at $I_0/I_d = $ e (*1*), 3e^2 (*2*) and 7e^4 (*3*).

applied external electric field, when the drift mechanism of nonlinearity dominates and a photoinduced waveguide is formed due to the screening of the field. As noted in [10], incoherent illumination of the sample, reducing the nonlinear response, makes it possible (apart from the applied external field) to influence the propagation of the spatial soliton.

In our case, when the ratio I_0/I_d is varied, the propagation of a light wave can be controlled by changing the diffusion potential $\varphi(x)$ of the internal field $E_\mathrm{sc}(x)$ of space charges with the density $\rho(x)$. At a relatively high intensity I_d, the stimulated scattering effect is predominant, and the scattering and localised propagation effects equally correspond to the average values of $I_\mathrm{d} \leqslant I_0$. Apparently, we realised this regime in [4, 5] at a wavelength $\lambda = 0.44$ μm and a beam power of ~1 mW. According to our calculations, for the Gaussian pump beam parameters $w_0 = 100$ μm and $I_0/I_\mathrm{d} = \mathrm{e}$ or $3\mathrm{e}^2$, the waveguide channel, which is formed in the illuminated region of the crystal, can support two (three) local normal modes, respectively [11], and the transfer efficiency of the pump beam power into the waveguide modes varies with changing the ratio I_0/I_d.

For the other part of the beam, the crystal region, where $\Delta n(x) < 0$, can be considered as a diffuser. In the case of interference of light beams, which occur on regular optical inhomogeneities induced by the pump beam, refractive index gratings are formed. These gratings diffract scattered waves in a positive and in a negative direction of the axis x. In the first case, scattered light is attenuated, and in the second case, scattered light is amplified. This mechanism of light-induced scattering was described in [12]. As a seed mechanism of this effect, the authors found that the light scattering is due to the crystal defects. A careful analysis shows also the role of regular inhomogeneities generated by the pump beam.

If $I_0/I_\mathrm{d} \gg 1$, the beam self-bending effect is most clearly manifested, which was discussed, for example, in papers [13–17].

3. Surface waves at the interface between a PR crystal and a dielectric

Let the polar axis of the crystal be oriented along the axis x. We consider the propagation of extraordinary polarised (TM) light along the axis z, which is directed along the PR crystal – dielectric (air) interface located in the plane $x = 0$ (Fig. 2a). The stationary solution for the field distribution of the surface wave $H(x,z) = A(x)\exp(-\mathrm{i}\beta z)$ in the absence of an applied external field, when the diffusion mechanism of nonlinearity dominates, can be obtained from the equation [2]

$$\frac{\mathrm{d}^2 A(x)}{\mathrm{d}x^2} + 2\gamma \frac{A^2(x)}{A^2(x) + A_\mathrm{d}^2}\frac{\mathrm{d}A(x)}{\mathrm{d}x} + k_\perp^2 A(x) = 0, \quad (6)$$

where $\gamma = k_0^2 n_2^4 r_\mathrm{eff}\varphi_\mathrm{B}$; $k_\perp = (k_0^2 n_2^2 - \beta^2)^{1/2}$; A_d is the effective amplitude of dark illumination ($|A_\mathrm{d}|^2 \sim I_\mathrm{d}$); $k_0 = 2\pi/\lambda_0$; and λ_0 is the wavelength of light in vacuum. Equation (6) is an oscillation equation with a nonlinear damping coefficient $\Gamma(x) = \gamma A^2(x)/[A^2(x) + A_\mathrm{d}^2]$. The coefficient $k_\perp$ determines the spatial oscillation frequency $K(x)$ of the amplitude $A(x)$ along the x axis:

$$K(x) = \{k_\perp^2 - \gamma^2 A^4(x)/[A^2(x) + A_\mathrm{d}^2]\}^{1/2}. \quad (7)$$

At $A^2(x) \ll A_\mathrm{d}^2$, $\Gamma(x) \to 0$ and equation (6) transforms into the equation of harmonic oscillations. In the case of $A^2(x) \gg A_\mathrm{d}^2$,

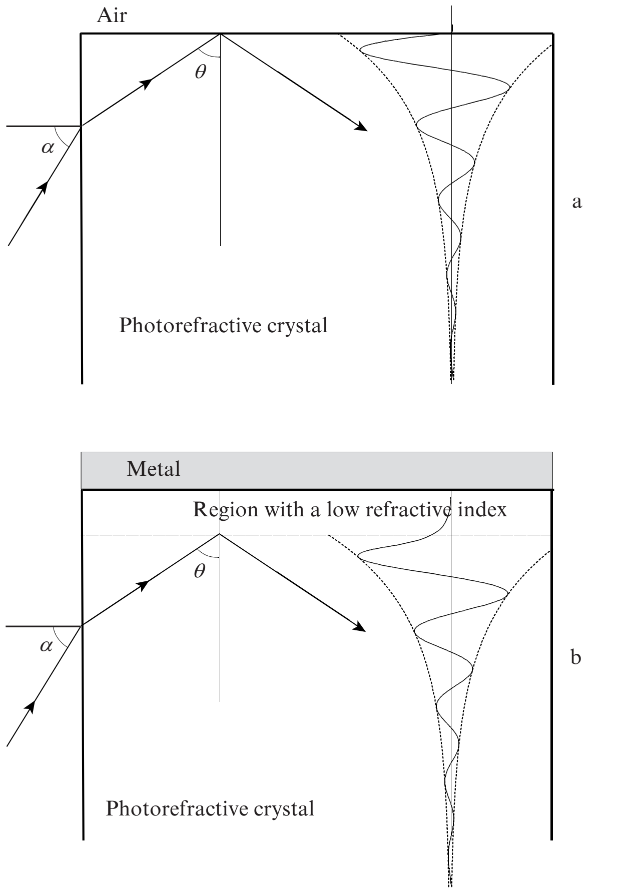

Figure 2. Scheme of excitation and propagation of a surface wave at the interface between a PR crystal and air (a) or metal (b).

$\Gamma(x) \sim \gamma$ and equation (6) is generally regarded as a linear oscillation equation with a constant damping coefficient. For example, Garcia Quirino et al. [1] present the solution that is obtained by neglecting the dark illumination and describes the surface waves, for which the spatial frequency is independent of x [$K(x) = \mathrm{const}$]. In this approximation and at $\gamma^2 < k_\perp^2$, the distribution $A(x)$ has the form of the interference pattern, which is formed by inhomogeneous light beams incident on and reflected from the surface. This wave has a characteristic oscillation period of the field $\Lambda = 2\pi/K$ and penetrates into the PR crystal to a depth $d = 1/\gamma$.

The surface wave propagation constant β is related to the angle of incidence θ on the interface of the exciting light by the expression

$$\beta = k_0 n_2 \sin\theta. \quad (8)$$

This case corresponds to the angles $\theta < \arccos[\gamma/(k_0 n_2)]$ and was discussed previously in [4]. The surface wave with an oscillating amplitude profile was observed at an oblique incidence of the focused light beam on the polished face of the crystal. The angle of incidence α related to the angle θ by the expression $\sin\alpha = n_2\cos\theta$ satisfied the condition $\alpha > \alpha_0$ [where $\alpha_0 = \arcsin(\gamma/k_0)$].

Let us consider in detail the case $\gamma^2 > k_\perp^2$. By neglecting the dark illumination, the amplitude profile in the crystal (at $x > 0$) is aperiodic [1, 4]:

$$A(x) = \exp(-\gamma x)[C_1\exp(Kx) + C_2\exp(-Kx)],$$

$$K = (\gamma^2 - k_\perp^2)^{1/2}. \tag{9}$$

In a dielectric (at $x < 0$), the amplitude of the surface wave has the form

$$U(x) = U_0 \exp(\gamma_d x), \quad \gamma_d = (\beta^2 - k_0^2 n_1^2)^{1/2}, \tag{10}$$

where n_1 is the refractive index of the dielectric. From the condition of continuity of the tangential components of the fields at the PR crystal – dielectric interface, we obtain the equalities

$$U(x)\big|_{x=0} = A(x)\big|_{x=0}, \quad \frac{1}{n_1^2}\frac{\partial U(x)}{\partial x}\bigg|_{x=0} = \frac{1}{n_2^2}\frac{\partial A(x)}{\partial x}\bigg|_{x=0}. \tag{11}$$

Taking into account (11) we derive from (10) and (9)

$$C_1 = U_0(1+a)/2, \; C_2 = U_0(1-a)/2, \; a = (n_2^2\gamma_d + \gamma)/K. \tag{12}$$

A surface wave with a nonoscillating amplitude profile can be observed only at very low grazing angles of the beam that excites this wave. Therefore, the angle of incidence α should be very small: $\alpha < \alpha_0$.

Figure 3a shows the profile $A(x)$ calculated by formulas (10)–(12) for $A_d = 0$, $\gamma = 0.125$ μm^{-1}, $k_0 = 14.28$ μm^{-1}, $n_1 = 1$, $n_2 = 2.36$, $\alpha_0 \sim 0.5°$ at different angles of α. When $x = x_m = [1/(2K)]\ln[(\gamma + K)(a-1)/(\gamma - K)(a+1)]$, the field amplitude of the wave has a maximum $A(x_m) = A_m$, a much larger than the field amplitude $A(0) = U_0$ on the surface $x = 0$, and when $x \to \infty$, the amplitude $A(x) \to 0$. It can be seen that the full width of the wave field distribution, determined by the half-amplitude, varies with the angle α, and this must be taken into account when optimising the surface wave excitation conditions.

When $A_d \neq 0$, equation (6) is solved numerically. Figure 3b shows the profile $A(x)$ calculated for the case $\alpha = 0.25°$ at different ratios A_m/A_d. The amplitude distribution is described by an aperiodic function only in a limited range $x_1 < x < x_2$, when the condition $A(x) > A_d$ is fulfilled [where $A(x_1) = A(x_2) = A_d$]. In the region $x > x_1$, where $A(x) < A_d$, there arise the oscillations of the field amplitude. At low levels of background illumination [Fig. 3b, curve (*1*)] the distribution of the wave field amplitude in a wide range of values of the coordinate x is almost identical to the distribution in Fig. 3a [curve (*2*)] obtained without the dark illumination. For curve (*2*), this range is much narrower, and for curve (*3*) (high intensity of background illumination), the oscillations of the wave field amplitude occur throughout the illuminated region of the crystal.

At a relatively low level of background illumination [$I(x) \propto |A(x)|^2 \gg I_d \propto |A_d|^2$], when the wave is assumed aperiodic, using (10) – (12), for a given angle of incidence θ we can determine the distribution of the surface wave amplitude, and then after substituting it in (2) we obtain the expression for the electrostatic potential

$$\varphi(x) = \varphi_B \ln[1 + A^2(x)/A_d^2] \approx \varphi_B \ln[1 + (U_0/A_d)^2$$
$$\times (\cosh Kx + a \sinh Kx)^2 \exp(-2\gamma x)]. \tag{13}$$

The distributions $E_{sc}(x)$ and $\rho(x)$ in this case can be presented in the form:

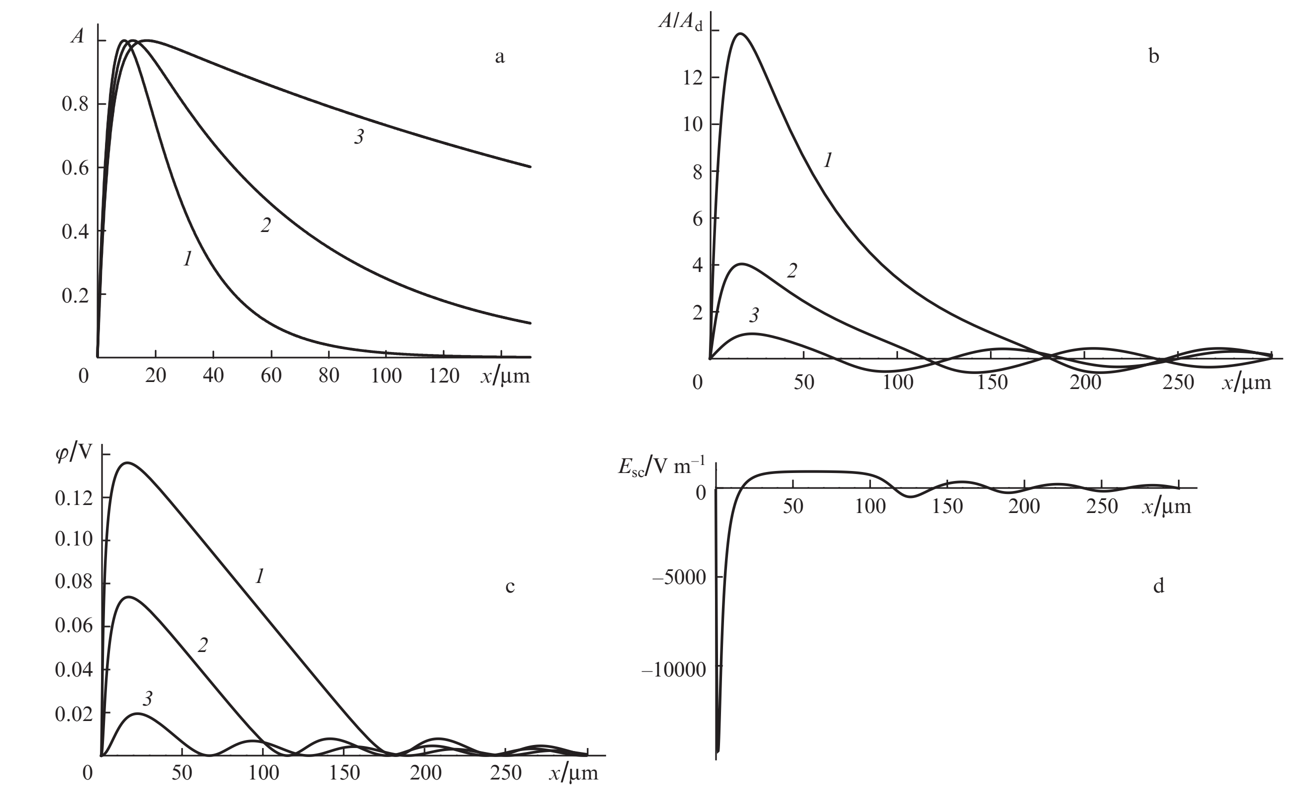

Figure 3. Profiles $A(x)$ of the surface wave at the PR crystal – air interface, calculated for $A_d = 0$, $\gamma = 0.125$ μm^{-1}, $k_0 = 14.28$ μm^{-1}, $n_1 = 1$, $n_2 = 2.36$, $\alpha_0 \sim 0.5°$ at $\alpha = 0.4°$ (*1*), 0.25° (*2*) and 0.125° (*3*) (a) and for $\alpha = 0.25°$ при $A_m/A_d = 14$ (*1*), 4 (*2*) and 1 (*2*) (b), and the profiles $\varphi(x)$, corresponding to the wave whose amplitude profiles $A(x)$ are shown in Fig. 3b (c), and the profile $E_{sc}(x)$, calculated at $A_m/A_d = 4$ (d).

$$E_{sc}(x) = -\frac{2\varphi_B A(x)}{A^2(x)+A_d^2}\frac{dA(x)}{dx}$$

$$\approx 2\varphi_B\left(\gamma - K\frac{a+\tanh Kx}{1+a\tanh Kx}\right), \tag{14}$$

$$\rho(x) = -2\varepsilon\varepsilon_0\varphi_B\left\{\frac{A(x)}{A^2(x)+A_d^2}\frac{d^2A(x)}{dx^2} - \frac{A^2(x)-A_d^2}{[A^2(x)+A_d^2]^2}\right.$$

$$\left.\times\left[\frac{dA(x)}{dx}\right]^2\right\} \approx 2\varepsilon\varepsilon_0\varphi_B\frac{(1-\tanh^2 Kx)K^2}{(1+a\tanh Kx)^2}(a^2-1). \tag{15}$$

When $x = x_m = [1/(2K)]\ln[(\gamma+K)(a-1)/(a+1)\times(\gamma-K)]$, the field amplitude of the wave has a maximum $A(x_m) = A_m$ and the electrostatic field $E_{sc}(x_m) = 0$. In the range $x < x_m$ ($x > x_m$), the field $E_{sc}(x_m) < 0$ ($E_{sc}(x) > 0$). According to (15) when the condition $a^2 - 1 > 0$ is fulfilled, we have $\rho(x) > 0$, and in the region $x > 0$ the positive charge q_0^* is concentrated. We assume below that the boundary of the crystal is nontransparent for the electric charge and the crystal is electrically neutral. As a result, near the crystal surface in a layer of thickness of the order of the Debye screening [7]

$$L_s = \frac{2\pi}{e}\sqrt{\frac{\varepsilon\varepsilon_0 k_B T}{N_{eff}}} \tag{16}$$

an electric charge $q_s \approx -q_0^*$ must accumulate. In this case, within the Debye screening layer the coordinate dependences $E_{sc}(x)$ and $\Delta n(x)$ will be different from the distribution obtained with the help of formulas (14) and (4). Obviously, solution (9) of equation (6), written without the effects associated with the accumulation of the screening charge, is valid only in the region of the crystal, located outside of this layer.

In cases where the wave cannot be regarded as strictly aperiodic, the distributions $\varphi(x)$ and $E_{sc}(x)$ can only be found numerically. Figure 3c presents the profiles $\varphi(x)$, corresponding to a wave whose amplitude profile $A(x)$ is shown in Fig. 3b. One can see that the electric potential is comparable to the potential resulting from the propagation of the Gaussian beam inside the crystal, and its maximum value (~0.135, 0.075 and 0.02) depends on the value of A_m/A_d.

Figure 3d shows the profile $E_{sc}(x)$ calculated at $A_m/A_d = 4$. The numerical values of the modulus $E_{sc}(x)$ are maximal in the vicinity of the crystal surface, in a relatively narrow layer of thickness of about 10 μm. In this layer, the nonlinear addition to the refractive index $\Delta n(x)$ is positive according to (4), and we can consider it as a waveguide layer. In a slightly deeper layer (buffer) of thickness 50 – 100 μm, the value of $E_{sc}(x)$ changes slowly and the corresponding value of $\Delta n(x)$ is negative. In the crystal region, located deeper than the buffer layer, the dependences $E_{sc}(x)$ and $\Delta n(x)$ have the form of quasi-periodic oscillations. This region of the crystal can be considered as the refractive index grating.

A nonlinear PR wave propagating along the surface of the PR crystal and linear dielectric can be considered as a Bragg waveguide mode [5]. This mode is formed due to total internal reflection of light at the interface of the PR crystal with a linear dielectric and due to Bragg reflection from the reflective index grating with layers arranged parallel to the interface in the PR crystal. It should be emphasised that at very low incidence angles ($\alpha < \alpha_0$) of the exciting beam on the input end of the crystal, the refractive index grating is formed by light only in those regions of the crystal, in which the intensity of the light wave is small compared to the intensity of the dark illumination.

4. Nonlinear PR wave in the metal-film coated crystal

Before considering the propagation of light near the PR crystal – metal interface, we will study some features of the metal–dielectric (semiconductor) contact. It is known that when the dielectric (semiconductor) has a contact with a metal, there appear potential barriers in the boundary layers, and the carrier concentration inside these layers may vary greatly compared with the values inside the crystal.

We consider the crystal to be an n-type semiconductor, in which all quantities depend only on the coordinate x along the normal to the contact plane. We will measure the potential $\varphi(x)$ from its value in the contact plane (at $x = 0$, see Fig. 2b). Then, when an external voltage u is applied, the boundary conditions have the form

$$\varphi(0) = 0,\ N(0) = N_c,\ \varphi(\infty) = u_c,$$
$$u_c = u_{c0} + u,\ N(\infty) = N_0, \tag{17}$$

where u_{c0} is the contact difference of the potentials in the case $u = 0$; N_0 is the concentration of electrons in the bulk of the crystal; and N_c is the boundary concentration of electrons. In the absence of the current, N_c is given by the characteristic of the contact:

$$N_c = N_0\exp(-u_c/\varphi_B). \tag{18}$$

The electron concentration obeys the Boltzmann law

$$N(x) = N_c\exp[\varphi(x)/\varphi_B]. \tag{19}$$

In this case the distribution of the potential specifying the distribution of the electron concentration in the steady state can be found by solving the equation [18]

$$\frac{d^2\varphi(x)}{dx^2} = \frac{eN_c}{\varepsilon\varepsilon_0}\left\{\exp\left[\frac{\varphi(x)}{\varphi_B}\right] - \exp\left(\frac{u_c}{\varphi_B}\right)\right\}$$

$$= \frac{eN_0}{\varepsilon\varepsilon_0}\left\{\exp\left[\frac{\varphi(x)-u_c}{\varphi_B}\right] - 1\right\}. \tag{20}$$

Consider the potential distribution in the case of an enriched contact layer ($u_c < 0$, and the absolute value is several times higher than φ_B). In the vicinity of the space charge of this layer $\exp(u_c/\varphi_B) \ll \exp(\varphi/\varphi_B)$ and equation (20) simplifies to

$$\frac{d^2\varphi(x)}{dx^2} = \frac{eN_c}{\varepsilon\varepsilon_0}\exp\left[\frac{\varphi(x)}{\varphi_B}\right]. \tag{21}$$

The solution to equation (21) has the form

$$\varphi_s(x) = -2\varphi_B\ln(1 + x/l_d),\ l_d = [2\varepsilon\varepsilon_0\varphi_B/(eN_c)]^{1/2}, \tag{22}$$

where l_d is the characteristic length. The distribution of the electric field is described by the expression

$$E_s(x) = 2\varphi_B/(l_d + x). \quad (23)$$

According to (23) the maximum of the field $E_s^{max} = E_s(0) = 2\varphi_B/l_d = [2eN_0\varphi_B/(\varepsilon\varepsilon_0)]^{1/2}\exp[(-u_c/(2\varphi_B)]$ is reached on the surface of the crystal.

Away from the contact one can expand the exponent in (20) in a series, and using only two terms of the expansion, expression (20) can be written in a simpler form:

$$\frac{d^2\varphi(x)}{dx^2} = \frac{\varphi(x) - u_c}{l_b^2}, \; l_b^2 = \frac{\varepsilon\varepsilon_0\varphi_B}{eN_0}. \quad (24)$$

In this case, the potential and the electric field vary exponentially:

$$\varphi_s(x) = u_c[1 - \exp(-x/l_b)], \quad (25)$$

$$E_s(x) = -(u_c/l_b)\exp(-x/l_b). \quad (26)$$

In the PR crystal bordering the metal, the emergence of the electric field $E_s(x)$ leads to the perturbation of the refractive index $\Delta n_s(x)$. Figure 4 shows the profile $\Delta n_s(x)$ obtained at $u_c = -0.2$ V, $N_c = 10^{16}$ cm^{-3} and $\varphi_B = 0.025$ V. The decrease in the refractive index Δn_s is most pronounced in the vicinity of the crystal surface (in the layer of thickness $l_d \approx 0.8$ μm) and reaches approximately -0.0003. At the same time, the thickness of the layer, in which a decrease in the refractive index exceeds 0.000015 in modulus, is much greater than l_d and is equal to about 30 μm.

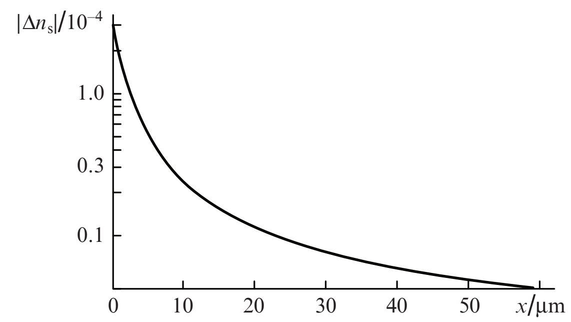

Figure 4. Profile $\Delta n_s(x)$, calculated at $u_c = -0.2$ V and $N_c = 10^{16}$ cm^{-3}.

This layer with a low refractive index may under certain conditions act as an optical barrier to the wave incident from the depth of the crystal to its surface coated with a metal film. Chen et al. [19] illustrate the use of an optical barrier to form an optical waveguide in a BiB_3O_6 crystal. To this end, implantation of He^+ ions deep inside the crystal makes it possible to create a layer with a low refractive index, which provides confinement of light in a narrow layer with a relatively high refractive index.

In our case, the surface wave in the metal-film coated crystal can be formed due to total internal reflection of light from the optical barrier, if the condition $\sin\alpha < (2\Delta n_s n_2)^{1/2}$ is met. According to our estimates, at angles of incidence of the exciting beam on the input end of the crystal, $\alpha > 2.15°$, surface waves with an oscillating intensity profile should arise, and when $\alpha < 2.15°$, subsurface waves appear. The near field wave

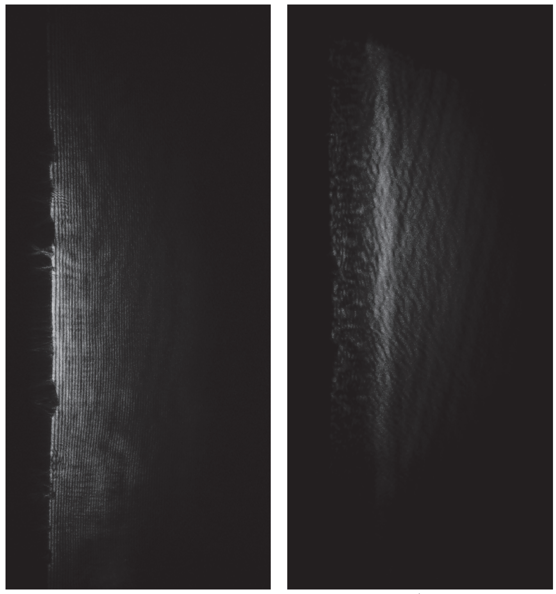

a b

Figure 5. Photographs of the output end of the crystal excited by a surface wave. The angle of incidence of the exciting wave is $\alpha = 4°$ (a) and 0.5° (b).

patterns (Fig. 5) obtained in the experiment at $\alpha = 4°$ and 0.5° confirm this fact.

5. Conclusions

To analyse the characteristics of photoinduced scattering in the nonlinear SBN-75 crystal and surface waves excited in its metal-coated surface, we have introduced the diffusion potential of the electrostatic field of space charges formed during the propagation of restricted light beams, and the potential arising at the PR crystal–metal contact.

Analysis of the electrostatic fields arising during the propagation of an aperiodic surface wave (in the absence of dark illumination), made on the basis of the method of images, has shown that when the wave propagates near the crystal surface bordering the dielectric, the formation of space charges in the illuminated region of the crystal should be accompanied by the accumulation of electrical charges of opposite sign in a narrow surface layer of thickness ~1 μm (of the order of the Debye screening length).

When the wave propagates near the surface of the metal-film coated crystal, the features observed in the distribution of the wave field, consisting in the appearance of a broadened emission band and in the shift of this band inside the crystal, are explained by the emergence of the layer with a low refractive index near the surface. We have shown that the thickness of this layer can greatly exceed 1 μm, and, under certain conditions, it can play the role of the optical barrier. The estimates of the angles of the exciting radiation ($\alpha \approx 0-2.15°$), in which these features manifest themselves most clearly, are in full agreement with those obtained previously in experiments ($\alpha \approx 0-2°$) [5].

Thus, our analysis has shown for the first time that the properties of the medium bordering the PR crystal can have a significant impact on the field distribution of the surface wave.

Acknowledgements. The authors thank V.V.Osiko for interest in the work. This work was partially supported by the Russian Foundation for Basic Research (Grant No. 10-02-01389-a) and the Russian Ministry of Education (State Contract No. 16.513.12.3019).

Appendix

Using the method of images [20] and introducing the fictitious charge $q_{\rm fic} = q_0^*(\varepsilon - \varepsilon_{\rm c})/(\varepsilon + \varepsilon_{\rm c})$ located mirror symmetrically (with respect to the plane $x = 0$) to the space charge q_0^*, $E_{\rm sc}^*(x)$ can be written in the form:

$$E_{\rm sc}^*(x) = E_0^* + \frac{1}{2\varepsilon\varepsilon_0}\left[\int_0^x \rho(\xi)\,{\rm d}\xi - \int_x^\infty \rho(\xi)\,{\rm d}\xi + q_{\rm fic}\right]$$
$$= E_{\rm sc}(x) + E_0^* + \frac{q_0^* + q_{\rm fic}}{2\varepsilon\varepsilon_0}, \tag{A1}$$
$$q_0^* = \int_0^\infty \rho(\xi)\,{\rm d}\xi, \quad q_{\rm fic} = \int_{-\infty}^0 \rho_{\rm fic}(\xi)\,{\rm d}\xi,$$
$$\rho_{\rm fic}(x) = \rho(-x)(\varepsilon - \varepsilon_{\rm c})/(\varepsilon + \varepsilon_{\rm c}),$$

where E_0^* is a constant; c is the dielectric constant of the medium adjacent to the crystal; and $\rho_{\rm fic}(x)$ is the fictitious charge density distribution.

When the surface wave propagates along the boundary $x = 0$, the electrostatic field established in the range $x > 0$ at the equilibrium of drift and diffusion components of the flux of the light-excited electric charge carriers must satisfy the condition

$$E_{\rm sc}^*(x) = -\frac{k_{\rm B}T}{q_{\rm e}}\frac{{\rm d}\ln[I(x) + I_{\rm d}]}{{\rm d}x},$$

i.e., coincide with the $E_{\rm sc}(x)$. This condition can be satisfied only with the accumulation of the charge $-q_0^*$ in a thin layer at the crystal – linear dielectric interface.

References

1. Garcia Quirino G.S., Sanchez-Mondragon J.J., Stepanov S. *Phys. Rev. A*, **51** (2), 1571 (1995).
2. Zhang T.H., Ren X.K., Wang B.H., et al. *Phys. Rev. A*, **76**, 013827 (2007).
3. Zhang T.H., Ren X.K., Wang B.H., et al. *J. Mod. Opt*., **54** (10), 1445 (2007).
4. Usievich B.A., Nurligareev D.Kh., Sychugov V.A., et al. *Kvantovaya Elektron*., **40** (5), 437 (2010) [*Quantum Electron*., **40** (5), 437 (2010)].
5. Usievich B.A., Nurligareev D.Kh., Sychugov V.A., et al. *Kvantovaya Elektron*., **41** (3), 262 (2011) [*Quantum Electron*., **41** (3), 262 (2011)].
6. Petrov M., Stepanov S., Khomenko A. *Photorefractive Crystals in Coherent Optical Systems* (Berlin: Springer-Verlag, 1991).
7. Bogodaev N.V., Ivleva L.I., Lykov P.A., Polozkov N.M., Osiko V.V. *Kvantovaya Elektron*., **27** (2), 170 (1999) [*Quantum Electron.*, **29** (5), 449 (1999)].
8. Feinberg J. *J. Opt. Soc. Am.*, **72** (1), 46 (1982).
9. Duree G.C., Shultz J.L., Salamo G.J., et al. *Phys. Rev. Lett*., **71** (4), 533 (1993).
10. Castillo M.D.I., Aguilar P.A.M., Sanches-Mondragon J.J., Stepanov S., Vysloukh V. *Appl. Phys. Lett*., **64** (4), 408 (1994).
11. Tamir T. (Ed.) *Guided-wave Optoelectronics* (Berlin: Springer, 1988; Moscow: Mir, 1991) Ch. 3.
12. Voronov V.V., Dorosh I.R., Kuz'minov Yu.S., Tkachenko N.V. *Kvantovaya Elektron*., **7**, 2313 (1980) [*Sov. J. Quantum Electron*., **10**, 1346 (1980)].
13. Feinberg J. *Opt. Lett*., **7** (10), 486 (1982).
14. Zozulya A.A., Saffman M., Anderson D.Z. *Phys. Rev. Lett*., **73** (6), 818 (1994).
15. Lyubomudrov O.V., Shkunov V.V. *J. Opt. Soc. Am*., **11** (8), 1403 (1994).
16. Aleshkevich V.A., Vysloukh V.A., Kartashov Ya.V. *Kvantovaya Elektron*., **28** (1), 64 (1999) [*Quantum Electron*., **29** (7), 621 (1999)].
17. Aleshkevich V.A., Vysloukh V.A., Kartashov Ya.V. *Kvantovaya Elektron*., **30**, 905 (2000) [*Quantum Electron*., **30**, 905 (2000)].
18. Bonch-Bruevich V.L., Kalashnikov S.G. *Fizika poluprovodnikov* (Physics of Semiconductors) (Moscow: Nauka, 1990) p. 221.
19. Chen F., Wang X., Wang K. *Opt. Mater*., **29**, 1523 (2007).
20. Tamm I.E. *Fundamentals of the Theory of Electricity* (Moscow: Mir Publ., 1979) Ch. 2.